Supplementary Information (SI) for
"Simple mathematical law benchmarks human confrontations"

Neil Johnson, Pablo Medina, Guannan Zhao, Daniel S. Messinger, John Horgan, Paul Gill, Juan Camilo Bohorquez, Whitney Mattson, Devon Gangi, Hong Qi, Pedro Manrique, Nicolas Velasquez, Ana Morgenstern, Elvira Restrepo, Nicholas Johnson, Michael Spagat and Roberto Zarama

Contents

1. Description of data-points in Figs. 1-3 and additional details of data sources

Data for the infant-parent dyads comes from our (Messinger group) laboratory experiments. Details of the experiment and laboratory conditions are given in the following papers: J.F. Cohn & E.Z. Tronick, Mother–infant face-to-face interaction: Influence is bidirectional and unrelated to periodic cycles in either partner's behavior. *Developmental Psychology* **24**, 386 –392 (1988); N. Ekas, J.D. Haltigan & D.S. Messinger, The Dynamic Still-Face Effect: Do Infants Decrease Bidding Over Time When Parents are Not Responsive? *Developmental Psychology* July 16, 1-9 (2012). Each experiment was performed separately, at a different time, and without communication between the participants in different dyads. An event is counted as starting when the infant presents a cry-face and ends when the infant stops presenting that cry-face. Each $(\log \tau_1, \beta)$ point corresponds to a unique infant-parent dyad in this laboratory experiment where the parent is instructed to temporarily refrain from interacting with the infant through positive affection etc. The infant (Red) attacks the parent in that it sporadically decides to present a cry-face to protest the lack of interaction with its parent (Blue). Millisecond scale digital monitoring records the time intervals between successive infant cry-face attacks (i.e. successive events) against the parent. The time-interval sequence for each dyad yields its own $(\log \tau_1, \beta)$ point in the plot. Since the infant-parent dyads involve different people, at a different place and time, it is remarkable that a linear relationship emerges in Fig. 2A.

Data for protests are obtained from the European Protest and Coercion Data Project undertaken by the University of Kansas, and compiled and provided by Prof. Ron Francisco from the University of Kansas. The data is public and can be downloaded from http://web.ku.edu/~ronfran/data/index.html. This is a coded dataset containing the day, action type, location, protest group and targets on protest and coercion in Europe. We took the following sets from the website: Poland 1980-1981, Poland 1982-1983, Poland 1984-1985, Poland 1986-1987, and Poland 1988-1989. This corresponds to the period prior to the fall of the Berlin Wall and the subsequent dissolution of the Soviet Union. The events are street protests by anti-Communist groups (Red) against the Polish government (Blue) prior to the fall of the Soviet Union. Each $(\log \tau_1, \beta)$ point corresponds to a different geographic location.

Data for the cyber-attacks are extracted digitally from the February 2013 report by MANDIANT on cyber attacks by a foreign, suspected Chinese, group (Red) against national infrastructure sectors (Blue). See www.mandiant.com.

Data for the predatory trading attacks are stock price data on the millisecond timescale (shown explicitly in charts on NANEX website www.nanex.net, with instructions for access below). The events correspond to predatory high-frequency traders/algorithms (Red) suddenly taking aggressive positions against slower market participants (Blue), triggering an ultrafast dip or spike in a particular stock price. Each $(\log \tau_1, \beta)$ point corresponds to a particular U.S. financial institution's stock. Data provided to us by NANEX, see www.nanex.net, and correspond to ultrafast events in the period prior to the 2008 global financial crash. We are extremely grateful to Eric Hunsader of NANEX for his help with this. The data can also be obtained manually by visiting the NANEX website and recording the times of the spikes and dips from the files available.

The instructions for accessing this open source data are as follows:

1. Go to http://www.nanex.net
2. Click on Nanex Research to access page http://www.nanex.net/FlashCrash/OngoingResearch.html
3. In column "Research" on left hand side, click "Micro Flash Crashes" to access http://www.nanex.net/FlashCrashEquities/FlashCrashAnalysis_Equities.html
4. This contains all the events used in the study.
5. As stated on this page, the links on this page contain "…ZIP archives for each year analyzed. Simply download the files, unzip and start viewing."
6. As examples, there are also 10 pages with 10 sample images from each year to view.
7. As stated, each chart contains a set of numbers in the upper left corner, which give the details for each. The meaning of these numbers is given on the website.

The datapoint for sexual violence against women comes from "The Power Laws of Violence against Women: Rescaling Research and Policies" by Karolin E. Kappler and Andreas Kaltenbrunner, PLoS ONE **7**, e40289 (2012). As stated by the researchers, their analysis uses data from the research study Health, Well-Being and Personal Safety of Women in Germany: Muller U, Schrottle M, Glammeier S (2004) Lebenssituation, Sicherheit und Gesundheit von Frauen in Deutschland. Eine reprasentative Untersuchung zu Gewalt gegen Frauen in Deutschland. BFSFJ, Bonn, 1.0.0, 13.04.2010, doi:10.4232/1.4193. BFSFJ website. Available: http://www.bmfsfj.de/ BMFSFJ/root,did = 20560.html, accessed 17 May 2012. As they state: "(quote).. It was the first representative survey on VaW [Violence against Women] in Germany, forming part of the national action plan published in 1999 by the German Federal Government to combat VaW. The representative study is based on 10,264 interviews, conducted nation-wide from February until October 2003 with women aged 16 to 85, residing in Germany". We consider sexual violence against women, since this is the closest variable to the notion of casualties, with the severity in this case measured as the number of cases per woman.

Some of the civil unrest/conflict data in Fig. 1A was obtained from Uppsala Conflict Data Program, http://www.pcr.uu.se/research/UCDP/ . It is geo-referenced data. Below are the identities of each of the points in Fig. 1A. The shade of color for each denotes the range of the number of victims:

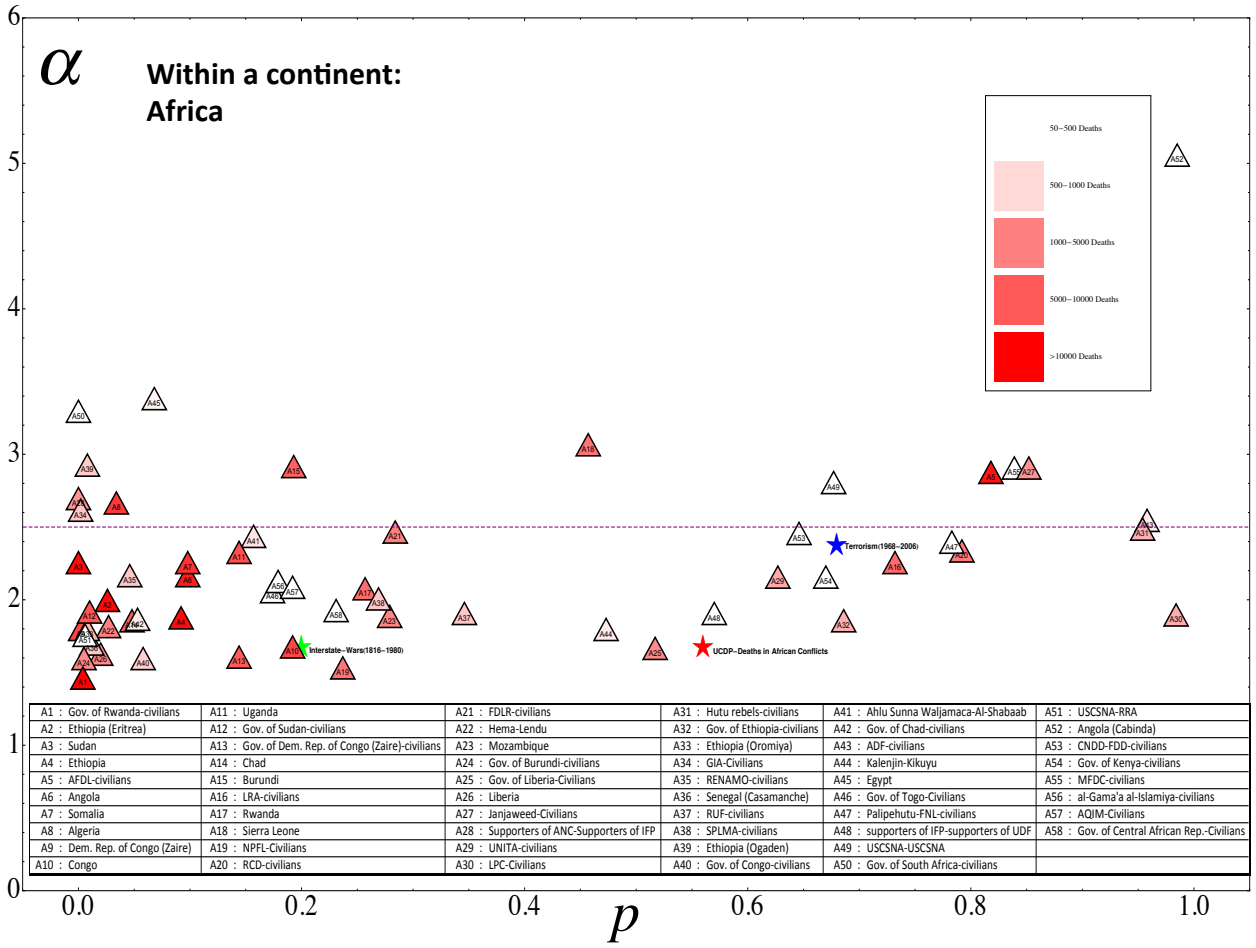

A1 : Gov. of Rwanda-civilians	A11 : Uganda	A21 : FDLR-civilians	A31 : Hutu rebels-civilians	A41 : Ahlu Sunna Waljamaca-Al-Shabaab	A51 : USCSNA-RRA
A2 : Ethiopia (Eritrea)	A12 : Gov. of Sudan-civilians	A22 : Hema-Lendu	A32 : Gov. of Ethiopia-civilians	A42 : Gov. of Chad-civilians	A52 : Angola (Cabinda)
A3 : Sudan	A13 : Gov. of Dem. Rep. of Congo (Zaire)-civilians	A23 : Mozambique	A33 : Ethiopia (Oromiya)	A43 : ADF-civilians	A53 : CNDD-FDD-civilians
A4 : Ethiopia	A14 : Chad	A24 : Gov. of Burundi-civilians	A34 : GIA-Civilians	A44 : Kalenjin-Kikuyu	A54 : Gov. of Kenya-civilians
A5 : AFDL-civilians	A15 : Burundi	A25 : Gov. of Liberia-Civilians	A35 : RENAMO-civilians	A45 : Egypt	A55 : MFDC-civilians
A6 : Angola	A16 : LRA-civilians	A26 : Liberia	A36 : Senegal (Casamanche)	A46 : Gov. of Togo-Civilians	A56 : al-Gama'a al-Islamiya-civilians
A7 : Somalia	A17 : Rwanda	A27 : Janjaweed-Civilians	A37 : RUF-civilians	A47 : Palipehutu-FNL-civilians	A57 : AQIM-Civilians
A8 : Algeria	A18 : Sierra Leone	A28 : Supporters of ANC-Supporters of IFP	A38 : SPLMA-civilians	A48 : supporters of IFP-supporters of UDF	A58 : Gov. of Central African Rep.-Civilians
A9 : Dem. Rep. of Congo (Zaire)	A19 : NPFL-Civilians	A29 : UNITA-civilians	A39 : Ethiopia (Ogaden)	A49 : USCSNA-USCSNA	
A10 : Congo	A20 : RCD-civilians	A30 : LPC-Civilians	A40 : Gov. of Congo-civilians	A50 : Gov. of South Africa-civilians	

Fig. S1. Details of datapoints in Fig. 1A of main paper text, for conflicts within a given continent. Each conflict is coded. Also shown are the results for global terrorism, interstate wars and deaths for events aggregated for all African conflicts.

In Fig. 1B showing a mix of countries across the globe, we also included datasets that we helped compile which list severity measured by actor, and also according to whether measured in terms of injuries or death. Our benchmark results can be seen to be robust to these changes in definition:

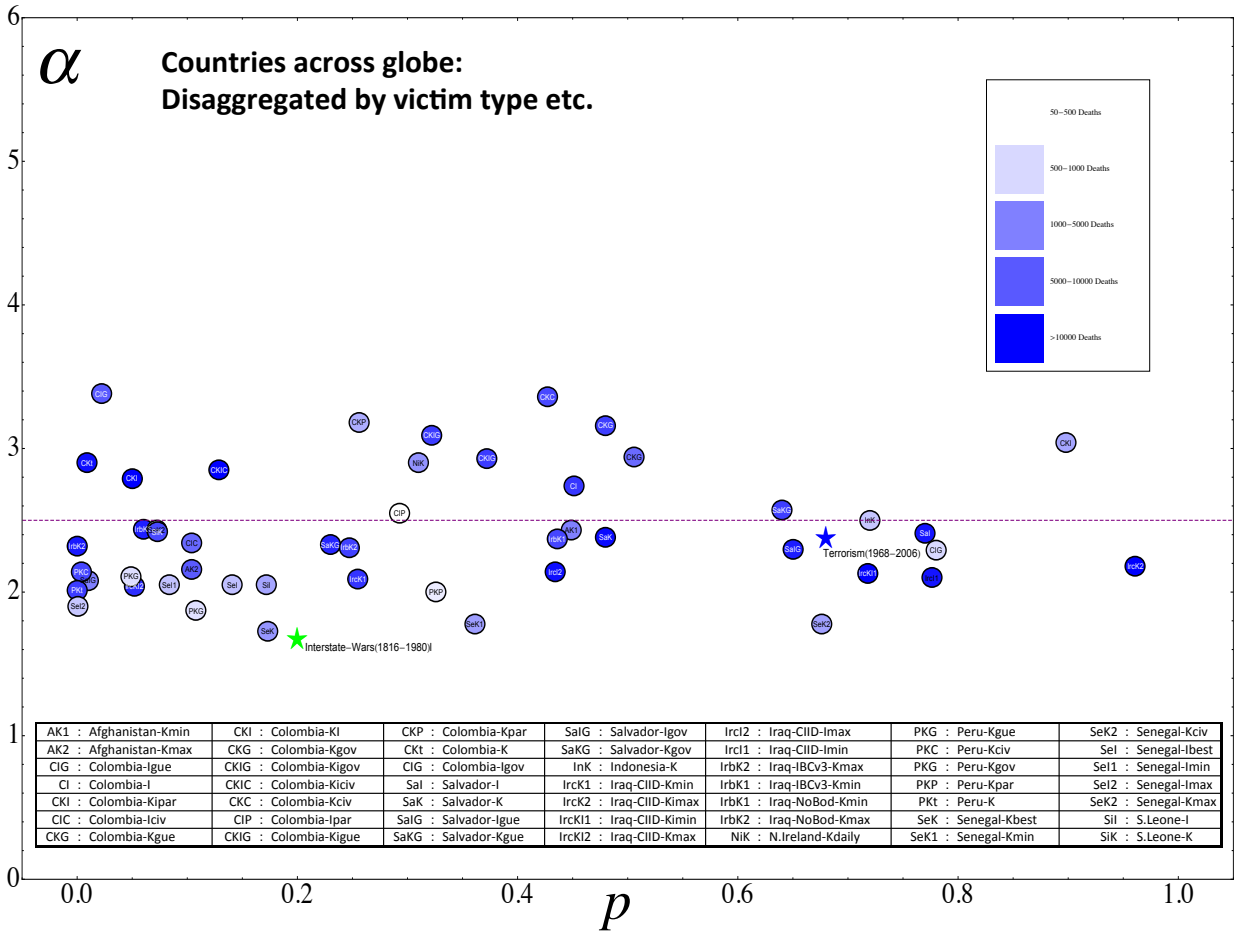

AK1 : Afghanistan-Kmin	CKI : Colombia-KI	CKP : Colombia-Kpar	SalG : Salvador-Igov	IrcI2 : Iraq-CIID-Imax	PKG : Peru-Kgue	SeK2 : Senegal-Kciv
AK2 : Afghanistan-Kmax	CKG : Colombia-Kgov	CKt : Colombia-K	SaKG : Salvador-Kgov	IrcI1 : Iraq-CIID-Imin	PKC : Peru-Kciv	SeI : Senegal-Ibest
CIG : Colombia-Igue	CKIG : Colombia-Kigov	CIG : Colombia-Igov	InK : Indonesia-K	IrbK2 : Iraq-IBCv3-Kmax	PKG : Peru-Kgov	SeI1 : Senegal-Imin
CI : Colombia-I	CKIC : Colombia-Kiciv	SaI : Salvador-I	IrcK1 : Iraq-CIID-Kmin	IrbK1 : Iraq-IBCv3-Kmin	PKP : Peru-Kpar	SeI2 : Senegal-Imax
CKI : Colombia-Kipar	CKC : Colombia-Kciv	SaK : Salvador-K	IrcK2 : Iraq-CIID-Kimax	IrbK1 : Iraq-NoBod-Kmin	PKt : Peru-K	SeK2 : Senegal-Kmax
CIC : Colombia-Iciv	CIP : Colombia-Ipar	SalG : Salvador-Igue	IrcKI1 : Iraq-CIID-Kimin	IrbK2 : Iraq-NoBod-Kmax	SeK : Senegal-Kbest	SiI : S.Leone-I
CKG : Colombia-Kgue	CKIG : Colombia-Kigue	SaKG : Salvador-Kgue	IrcKI2 : Iraq-CIID-Kmax	NiK : N.Ireland-Kdaily	SeK1 : Senegal-Kmin	SiK : S.Leone-K

Fig. S2. Details of datapoints in Fig. 1B of main paper text, for conflicts in different countries and continents. Each conflict is coded, with the data corresponding to different measures of severity (i.e. killed, injured, also maximum and minimum estimated body counts). Also shown are the results for global terrorism and interstate wars.

All the civil unrest/conflict datasets tend to use the same common-sense definition of an 'event' as an occurrence of an action involving a group of armed actors that cannot be partitioned into any smaller set of actions, can be distinguished from other such events, is carried out by at least one recognized group in a conflict, involves a number of casualties being reported, and there is some broad strategic description that can be given, i.e. weapons used, or military objective, or general identity of units involved. For the Afghanistan conflict we used a dataset integrating data provided by Marc Herold of the University of New Hampshire (http://pubpages.unh.edu/~mwherold/) with data from icasualties.org (http://www.icasualties.org/) and the ITERATE (http://www.ciser.cornell.edu) terrorism database. The Iraq data, like the Afghanistan data, is an amalgamation of three separate data sets that record violent events in Iraq. These data-sets are Iraq Body Count (IBC, http://www.iraqbodycount.org/), icasualities.org and ITERATE. Ultimately, all the data comes from multiple sources that can be grouped into three broad categories; real-time media databases, official (government and nongovernmental organization (NGO)) reports, and academic studies. Some sources use real-time media monitoring of the stream of stories about violent events from newspapers, web-sites and television. These databases typically monitor a range of media channels and employ filters to cross-check different stories for accuracy. For the

Peruvian conflict, data is built from the report published by Truth and Reconciliation Committee (TRC): *http://www.cverdad.org.pe/ingles/ifinal/index.php*. The data for Sierra Leone comes from the academic work of Macartan Humphrey of Colombia University: *http://www.columbia.edu/-mh2245/* . The data source for the Northern Ireland conflict is the research of Malcolm Sutton: *http://cain.ulst.ac.uk/sutton/* which itself uses a large number of sources.

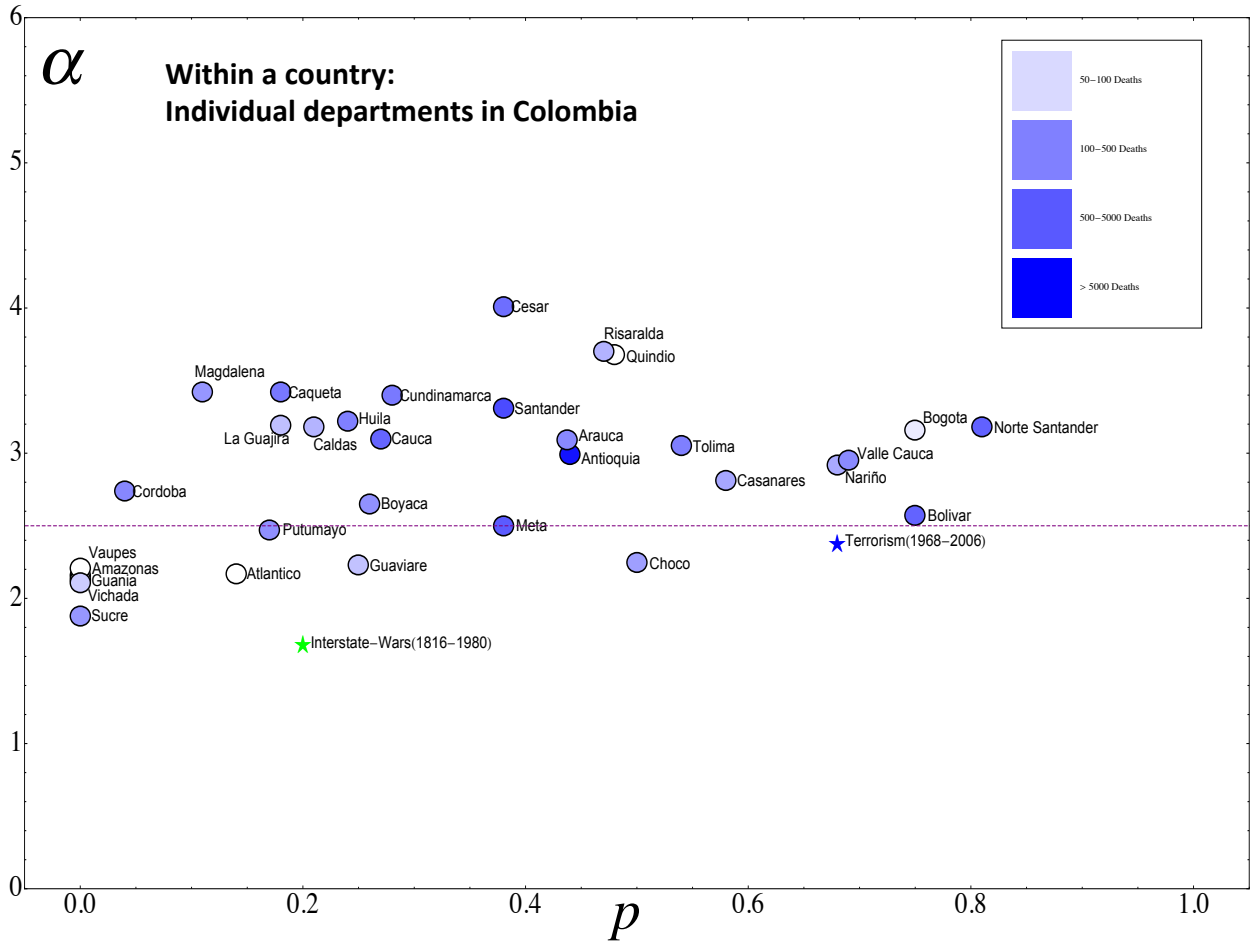

Fig. S3. Details of datapoints in Fig. 1C of main paper text, for conflicts in different political departments within a given country (Colombia). Also shown are the results for global terrorism and interstate wars.

The data used for different Departments within Colombia, above, are obtained from the Colombian Conflict Database, provided to us by the Conflict Analysis Resource Center-CERAC. The dataset contains the type of victim, the date and location of people killed or injured in the Colombian conflict, from 1988 to 2006. We took the insurgent guerrilla FARC as the Red side and the Colombian government as the Blue side. See *The Severity of the Colombian Conflict: Cross-Country Datasets versus New Micro Data* (J. Restrepo, M.Spagat and J. Vargas), Journal of Peace Research **43,** 99-115 (2006). Each point occurs in a separate geographical location (i.e. a separate Department).

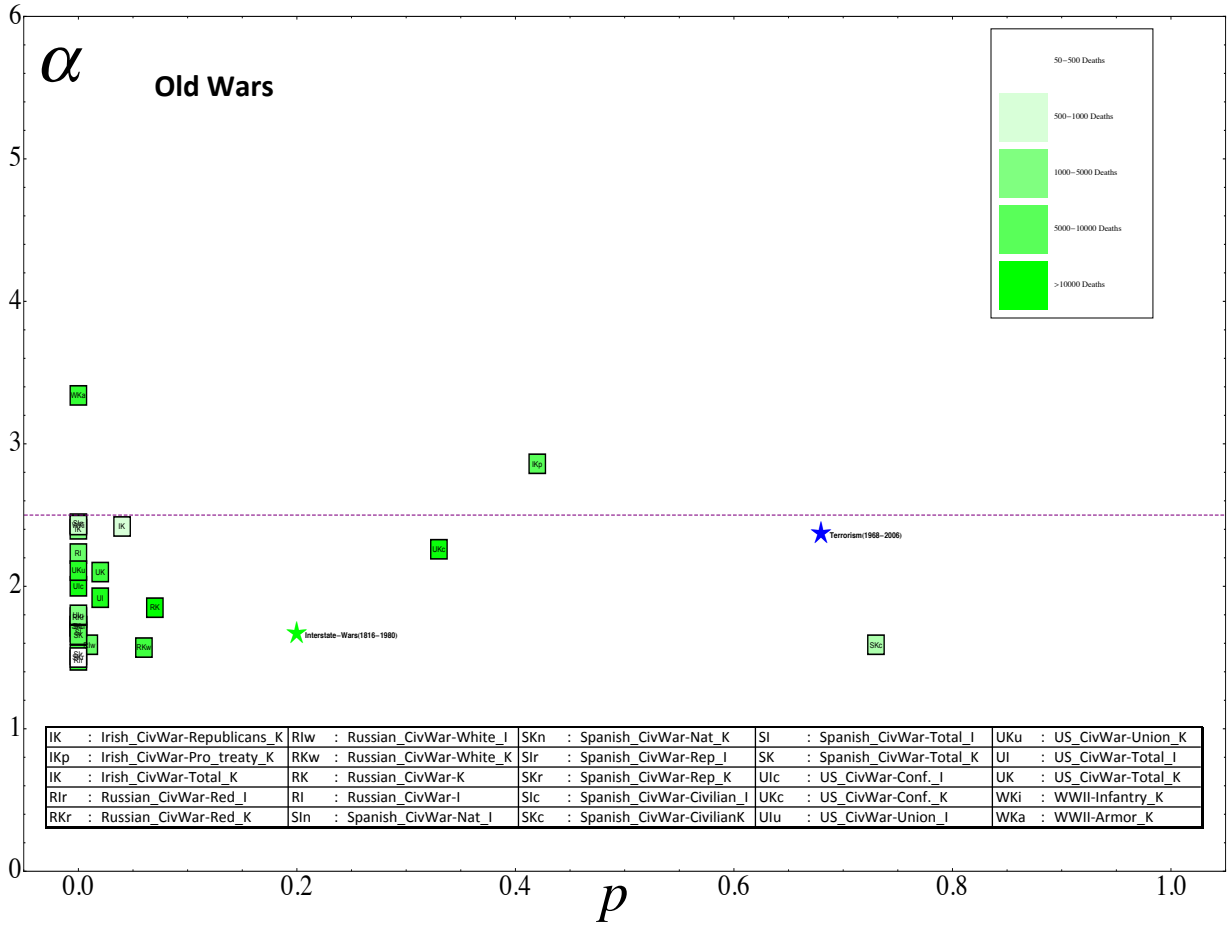

Fig. S4. Details of datapoints in Fig. 1D of main paper text, for more conventional wars. 'K' corresponds to numbers killed, and 'I' corresponds to numbers injured. Also shown are the results for global terrorism, and the value for all interstate wars aggregated between 1816-1980.

For the older data on the American and Spanish civil wars we use the academic work of Ron Francisco of the University of Kansas who, in turn, relies on historians accounts (http://web.ku.edu/~ronfran/data/civilwars/index.html).

The comparative data in Fig. 1D for suicides, accidents, homicides etc. is obtained from Medicina Legal in Colombia, and measures deaths from the various causes in the capital city Bogota. The range of corresponding exponent values α is effectively a continuous strip in Fig. 1D showing the range over which the α values vary as different criteria for severity are applied.

To give an idea of how close to 2.5 the values are in Fig. 1, the following list takes the α values in a particular plot, and calculates the mean value and the standard deviation, respectively:

Fig. 1A Africa	2.23635	0.6311
Fig. 1B (across the globe)	2.5082	0.4249
Fig. 1D (old wars)	2.0850	0.5067

More details about the research underlying the PIRA network analysis (Fig. 1D inset of the main paper) are given in P. Gill, J. Lee, K. Rethemeyer, J. Horgan and V. Asal. (*in Press*) "Lethal Connections: The Determinants of Network Connections in the Provisional Irish Republican Army, 1970-1998". *International Interactions* (2013).

The data for Fig. 3 are obtained from the above mentioned sources, and identities are as shown below:

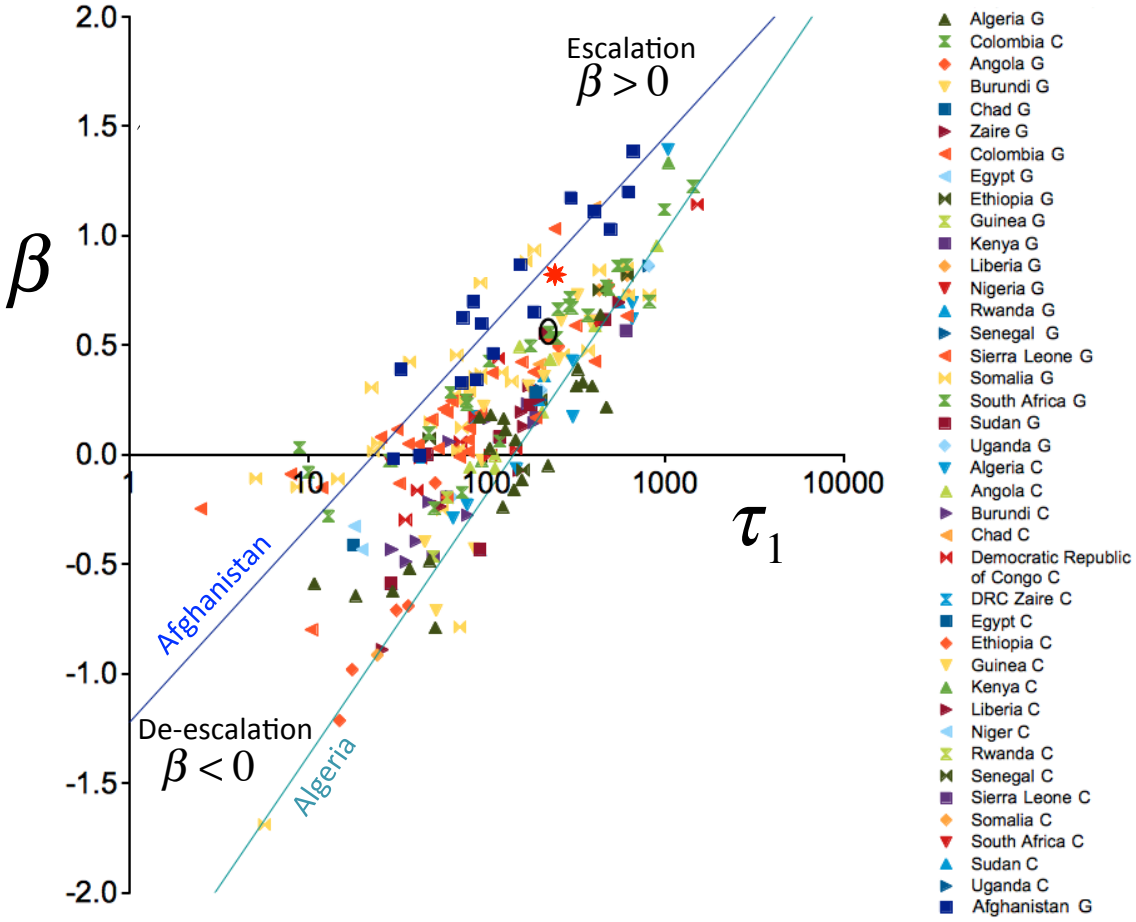

Fig. S5. Details of datapoints in Fig. 3 of main paper text. In the key, 'C' means civilian casualties inflicted by Red, while 'G' means government (army, state security) casualties inflicted by Red.

Figures 2 and 3 therefore span a wide spectrum of human confrontations: They show a progression from individual face-to-face confrontations in an otherwise affectionate relationship (Fig. 2A), to real-space non-violent and violent group-level political confrontations (Fig. 2B and Fig. 3), to cyber-based economic confrontations (Fig. 2D), and in Fig. 2C the example of a clandestine international Red entity of unknown size and origin carrying out cyber-attacks (events) against another country's Internet-based infrastructure (Blue).

In Figs. 2 and 3, we define the time interval between events as the time between the end of the previous event and the start of the next. For all the systems except some of the street protests, and the baby cry-face, the events (i.e. attacks) are essentially over in one timestep. Street protests and baby cry-faces can last several timesteps – hence, given its definition, the time interval is measured between the end of the previous protest/cry-face and the start of the next.

2. Data file description

Examples will be provided online as Excel files. For illustration, below we present a snapshot of the format for the timings analysis in Figs. 2 and 3. Each domain is a separate sheet and the dyads are columns. Each row in a given dyad contains a time interval between consecutive events, listed sequentially from top to bottom in a timescale of choice. For example for the insurgency, an event is a day in which Red attacked and killed Blue members, so the time interval is measured in days. The choice of scale of the time interval is not important for the analysis since the power-law curve is independent of scale (i.e. multiplying the time interval by a given factor affects both sides of the power-law progress curve equation equally and so does not change the corresponding α value). The case below is for Fig. 2D as illustration:

Fig2D

MS	GS	WFC	JPM	MET	BAC	BSC	LEH	C	AIG	MER	BK	PRU	GNK	POT	GE	BAC-PR-H	AXP	FCX	MOS
1.158517072	63.81986921	44.9987526	584.9597836	181.7830677	84.01114988	2.982996817	2.999006944	4.996764468	0.002674479	4.09203125	6.747346933	111.2528747	41.08205006	111.0123941	196.020228	15.10138079	12.78541638	14.17182002	1.994584491
97.73600231	98.21506481	16.99855671	30.80211545	3.999958044	432.1581557	0.040596065	0.987032408	0.006881944	184.118627	9.799301505	64.02733681	0.747340567	1.156728877	115.1504005	345.9639965	5.758392361	44.01541869	0.808844907	5.192103877
0.240689815	7.739822049	24.19832957	4.995875	231.0051615	23.81025926	0.158164931	6.014578704	1.988903356	42.14326563	88.14396962	14.08407841	30.04116464	3.900007523	145.0264907	349.9738151	4.161800637	196.2221991	56.02557726	11.80761111
153.7679497	0.999975116	12.83355093	14.19436863	0.005547164	6.162446181	0.988927083	0.184037616	147.0659071	10.74609057	69.8678206	2.015092593	62.09362066	1.947789641	14.90979745	67.01087963	24.04662066	35.8301195	113.9903206	281.9883559
62.15327865	27.26289063	11.99975289	0.072709201	0.007875	25.03946267	0.032789641	0.81908015	20.94047078	0.084887442	0.002436632	0.045350694	1.991454572	11.97115943	21.89252778	0.989390336	4.990503762	250.9369155	7.010854167	84.23217535
7.838138889	53.79648582	147.2624557	46.73349479	0.023531829	114.989066	1.031830729	3.98562934	18.99381047	0.035709491	0.033990451	0.057198206	3.073245081	6.989850694	1.121203125	0.021666667	2.921065394	26.98708131	142.9755723	124.0183087
29.00127604	66.13501591	0.91827662	2.07408912	2.202185764	11.8130489	6.764866319	14.0092853	55.06823814	0.129206308	0.004349537	0.018996528	0.012867766	0.172043981	76.10713686	0.978811632	18.99572685	2.111490162	0.005120081	14.75069097
0.00165162	24.85634491	6.819445602	92.92556655	5.958181134	0.028750289	0.223418981	14.04345428	1.93296412	288.7569363	55.03219502	2.759278646	0.001966146	2.924728009	63.77060069	1.16788397	13.1246276	10.88831858	8.051647859	14.12278414
0.997838831	34.9458912	1.998195023	25.00234722	2.047195023	42.95775492	25.74819878	29.17587529	4.997688657	4.989171296	30.94084288	0.244461806	0.045186343	0.070182581	4.036011863	0.859150463	0.985491319	0.183869502	57.15475289	29.87469502
12.00027922	2.07009838	62.07990249	0.018417535	2.784243924	100.0028556	8.195317708	15.77164497	0.170702546	2.257896123	64.23238079	0.994909722	0.005251447	41.79594763	2.196898148	0.091522569	4.806274595	1.980870081	15.78746007	0.043498553
9.252925636	0.932778646	8.09785272	0.007856192	0.042521412	17.26583391	56.07025608	40.99951678	0.837201678	28.73205324	11.75547251	0.746038773	0.997828414	33.00466667	0.028808449	0.015143518	0.129200232	0.8771875	122.264849	3.989692708
38.76647946	3.009609664	4.979398437	0.975577836	0.122204861	9.733269676	27.93024682	36.08130208	1.037206887	1.004116319	9.021542535	0.122719039	1.746916667	77.22660417	0.762900463	3.106355903	20.90172396	3.963471354	6.847555556	0.01921412
0.005860532	1.128863715	0.038901331	7.031642361	0.006201678	0.010980613	41.81107581	3.915629919	0.149442708	0.21361169	5.975985822	0.871048322	0.010414352	0.003810764	4.243612558	0.757717882	2.95747772	0.03967853	50.88544589	0.002294271
0.034693866	0.833082465	0.068782118	1.968113715	1.815381945	5.990348958	6.011317419	8.195836806	0.009398148	3.873883102	5.989713831	0.224205151		49.80048698	2.737472511	1.014156539	0.026195313	0.09074566	5.010447049	1.14519213
0.205823785	103.2393837	5.740903067	0.008281539	1.01119184	1.009551215	35.98435995	43.80849508	1.946690683		0.03373206	0.783489294		78.03998698	3.036646123	4.993847801	0.030841724	0.011487847	0.990540799	0.006976562
0.733475405	10.95250752	3.254915509	28.25481134	0.021033276	0.002756366	6.105015914	0.016654514	0.001708912		0.017177083	0.116958912		19.94682118	2.986700521	0.111266204	1.007381655	0.020314815	1.017254619	0.810981192
0.008018808	17.77974045	0.771427951	23.9981276	0.040280382	0.985430845	0.03100434	2.982645833	0.004164641		0.200668403	0.121684317			0.159650174	0.053267361	4.049397569	0.832970197	0.013478588	0.249945602
0.0960761	44.00024248	0.127292535	1.00156713	0.027989294	0.054240162	0.957621528	0.036977431	0.040081597		5.747439525	2.77433044			0.072959491	0.006560185		0.243572049	1.055583333	0.753773148
0.04039294	0.001818866	0.045687789	1.91045978	0.066451678	3.186064815	0.017802662	0.050319155	0.019065104		2.00176794				3.802790799	0.005060764		0.017260706	0.924978299	0.239803241
0.006591435	4.248627894	0.044916667	0.075674768	0.013965857	0.759626736	0.025017072	0.020173611	0.011916956		41.99749161				0.198065104	0.002130498		0.855605613	0.2442989	
0.066606694	0.771608218	0.009825231	3.986319734	0.006464699	0.036291956	0.016381945	0.003646412	0.009438657		0.001539931				0.999558449	0.003326389		0.060776042	2.742833912	
0.021177951	0.179008102	2.737856771	2.961512732	0.042613715	0.005760995	0.027172743	0.035992766	2.759997974		0.265572049				0.756787037	0.011537616			0.011761574	
0.027387442	0.872206308	0.009251447	0.802354167	0.009743634	0.226065972	1.828787326	0.00480816	0.054034144		3.751030382								0.240031539	
0.735147859	0.006064815	0.012623264	0.039327546	3.979440683	0.741822917	0.004764178	0.052722801	0.036685764		1.182134838								0.010230614	
0.00799566	0.006462095	0.009099826	2.976178819	0.016117477	1.991236401	0.149131944	0.042563657	0.173920718		0.982187211								2.737643229	
0.003319155	0.033450521	0.001427373	0.16620081	0.004880498	25.00160156	0.08343316	0.001730903	0.996147859		0.073579282								0.036215856	
0.030741609	0.00675434	0.094657986	0.056256944	0.004650463	0.999369502	0.017472801	0.015708044	0.739508102		1.743186053								4.964417824	
0.032620081	0.014457755	0.008887732	2.765495081	0.735687789	27.00002344	0.732078704	0.7339864	0.033624132		10.17668634									
0.06490625	0.057911748	0.015719618	0.231127604	0.13735821	1.04110706	0.005738136	13.04566782			0.002432581									
0.049587384	0.015042245	0.038206019	0.797489873	0.051172164	1.955638889	0.004538773	0.181468171			0.00472309									
0.036283275	0.793894097	0.03615191	0.174198785	0.001445891	14.26269358	0.001686632	57.82981568			0.010490741									
0.008357639	0.142674479	0.77184838	0.031001157	0.039191551	0.002019387	0.001797743				0.001729745									
0.006971643	0.013322049	0.074688079	2.761080729	0.013784144	2.73744213	0.006988426				1.906985532									
0.004327546	0.050086516	0.045408565	0.008499711	0.01786603	0.020784143	0.002782407				2.163841724									
0.004740741	0.009247396	0.012673032	0.250412037	0.004804109	0.010951389	0.007099537													
0.006156829	0.006769097	0.003800347	0.005598669	0.733448785	0.001435764	0.00438397													
0.747941262	0.022761285	0.02226331	0.733360822	0.010030093		0.003996238													
0.018253183	0.752542245	0.02048206	0.011718461			0.009431713													
0.005981482	0.001390046	0.01590625	0.010600116																
0.009942419	0.017838831	0.046689815	0.009685185																
2.958390625	0.153083623	0.003964989	0.0676386																
2.042594618	0.038146412	0.016271991	0.161350694																
0.21847309	2.785728588	0.739863715	0.740722222																
1.784964699	0.211302951	0.008189236	0.007484664																
3.130020544	3.798438368	0.006407118	0.003786169																
0.002811632	3.041089699	0.045190972	0.039734664																
0.002083912	0.134482928	0.001846065	0.103569445																
0.08499103	0.065786169	0.062442419	0.013654224																
0.769842303	0.015344618	0.063067708	0.039996817																
0.152073785	1.870748264	0.07366522																	
0.815100984	0.041000868	0.003045139																	
0.165347222	0.068830151	0.001683738																	
0.007002315	0.013933738																		
2.042650752	0.749024305																		
2.782305556	1.155109664																		
0.012384259	2.836375																		
0.011232928																			
0.004225116																			
0.17823785																			
0.799538484																			
0.017789641																			

Fig. S6. Snapshot of the data used in the analysis of the main paper, specifically in producing Fig. 2D.

3. Lack of systematic correlation between severity and timing

This can be seen from our datasets, however as illustration below we show that the exponent value α does not shift in a systematic way over time. The figure is obtained by dividing each confrontation up into four equal periods, without any prior knowledge of the resulting α value or goodness-of-fit:

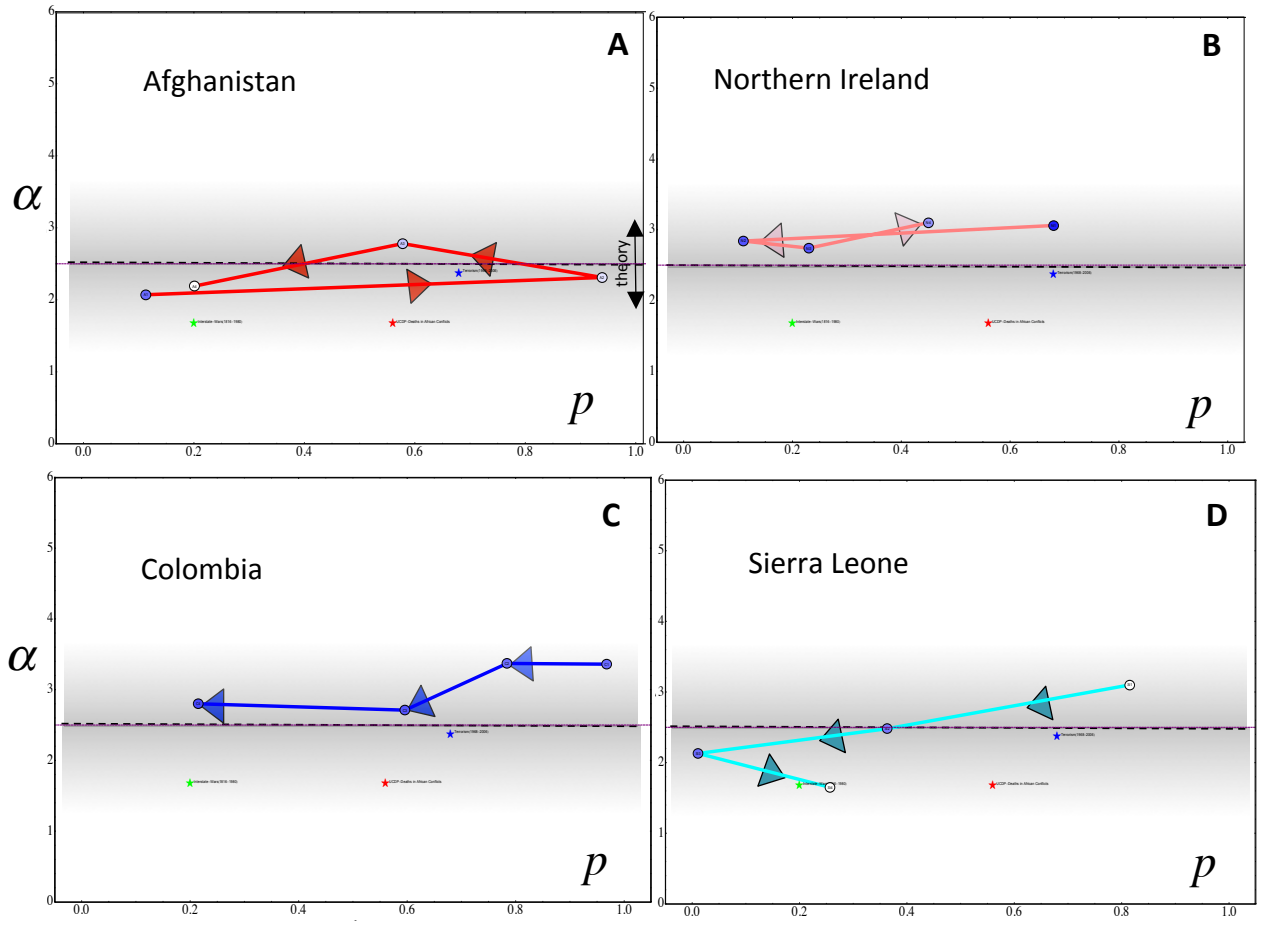

Fig. S7. Demonstration that severity and timings do not show systematic correlation. Examples chosen from four Red-Blue conflicts. The progression of values for four successive periods in time is shown. Same conclusion concerning lack of severity-timing correlation, holds for other choices of periods.

4. Residuals for best-fit curve for timings

Below we show a typical example of the best straight line fit through the empirical timings data on a log-log plot, for Magdalena in Colombia which is shown as a black oval in Fig. 3 of the main paper and occupies a position near the middle of all the data-points (see Fig. 3). On right below is the distribution of these residuals (top) confirming their near-Gaussian nature, and also a plot showing their lack of correlation (bottom). Both these observations are consistent with the requirement of having i.i.d. Gaussian distributed residuals, as claimed in the main paper.

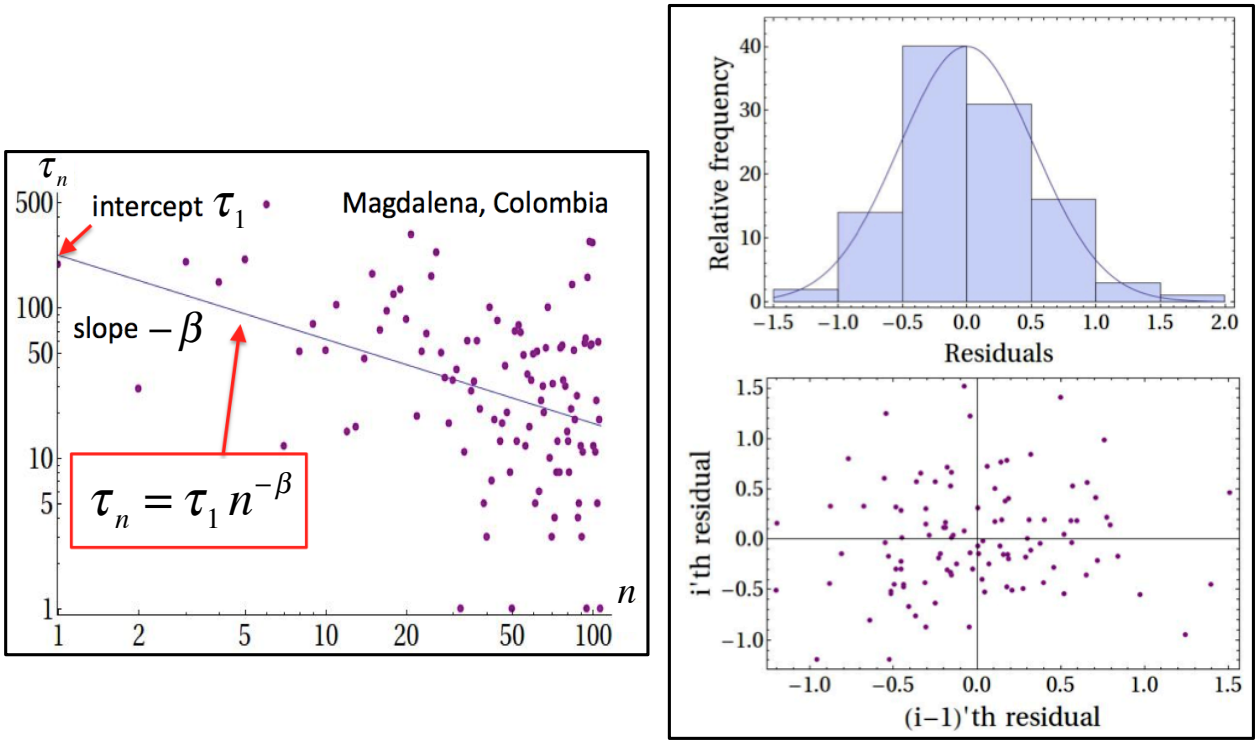

Fig. S8. Demonstration of power-law fit to trend in inter-event timings. Left panel shows the fit, right panel shows the properties of the residuals with (top) near Gaussian distribution and (bottom) lack of serial correlation as required.

5. Demonstration that linear dependence relationship for timings is non-trivial

We demonstrate below the non-trivial nature of the benchmark linear dependence for timings, by comparing to (a) real data from a real-world experiment where there is no active Blue opponent, and (b) model with randomized version of the data.

(a) Real data with no active Blue opponent:

Anyone engaged in a completing a particular task (i.e. facing an effectively static Blue) such as proof-reading, solving a puzzle, or purchasing something online, does not have to worry about that task (i.e. Blue) intentionally resisting completion. In panel B of the figure below, we summarize Crossman's classic results showing that for a given type of task (e.g. proof reading), each subject exhibits his/her own escalation rate and intercept. (See Crossman, E.R.F.W. A theory of the acquisition of speed-skill. *Ergonomics* **2**, 153-166 (1959)). The lack of a generic dependence between the two parameters is no surprise given the heterogeneity of humans (Red). Panel C shows that this lack of any linear dependence also arises for humans completing passive cyber tasks, specifically the navigation of different websites. Data from Johnson, E., Bellman, S., & Lohse, G.L. Cognitive Lock-In and the Power Law of Practice. *Journal of Marketing* **67**, 62-75 (2003):

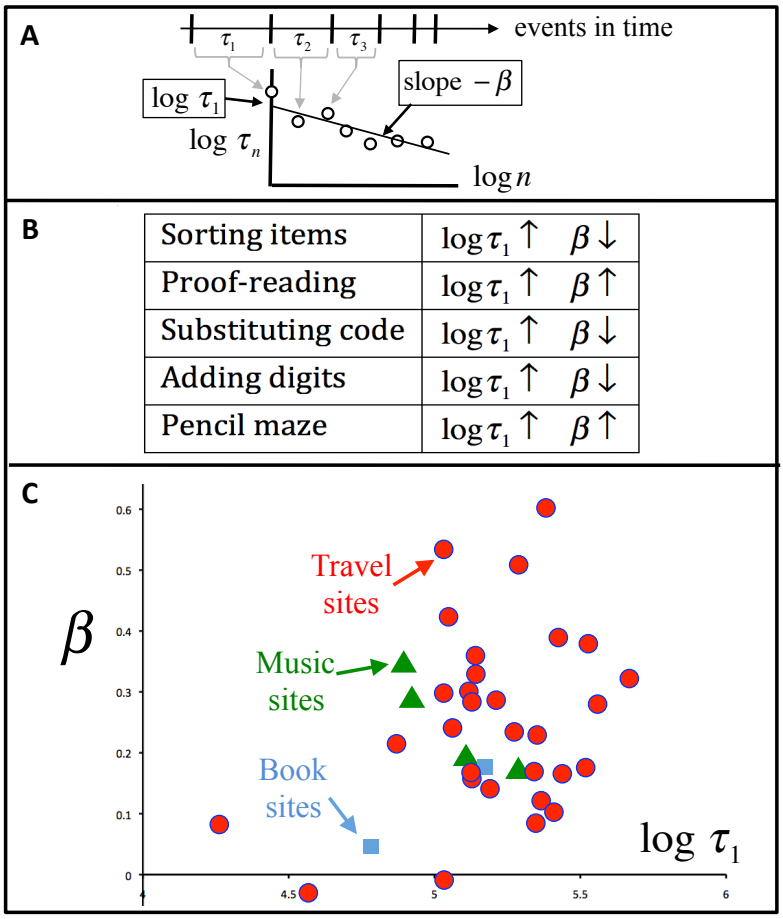

Fig. S9. Benchmark signature for timings disappears in one-sided activities (i.e. no active Blue). Top: fitting procedure. Middle: existing empirical results in the literature for passive tasks. There is no systematic relationship between τ_1 and β, in stark contrast to Figs. 2 and 3 of the main paper. Bottom: results for one-sided activity of searching Internet sites. Again there is no systematic relationship between τ_1 and β, in stark contrast to Figs. 2 and 3 of main paper. Data-sources given in SI text.

(b) Randomized data

Our method of adding stochasticity (randomness) to the event times, and hence generating a null model which we use to further investigate if the linear-dependence happens by chance, is as follows:

1. For each dyad i, calculate the total time T_i as the time between the first event and the last event.
2. For each i, take the number of events n_i and divide by T_i. This gives the probability p_i of an event per unit time for that dyad.
3. Generate a random series by considering an event at each timestep using probability p_i from step 2. Generate a total number of events n_i for each dyad. Hence the synthetic time-series we produce are conditioned on having the correct number of events, and also the correct duration on average. Choosing to preserve the correct duration, and have the correct number of events on average, leads to similar conclusions.
4. Calculate β and $\log \tau_1$ from step 3 for each dyad i.
5. Repeat steps 1-4 many times in order to get a set of simulated β vs. $\log \tau_1$ plots.

6. For each one of the simulated β vs. $\log \tau_1$ plots in step 5, calculate the R^2 of the β vs. $\log \tau_1$ best-line fit.

7. Calculate the mean and standard deviation for the R^2 distribution obtained in step 6. We find empirically that this distribution is approximately Gaussian: $N(\mu,\sigma)$

8. Using the distribution of the R^2 from step 7, estimate the p-value as the probability of getting a value of R^2 equal to, or greater than, the empirical value given by R^2_{real}. The values for the five domains we consider are as follows:

Fig. 2A p=0.0089 R^2_{real}=0.74 R^2_{random}=0.36

Fig. 2B $p = 5.7\times10^{-5}$ R^2_{real}=0.82 R^2_{random}=0.38

Fig. 2C p=0.036 R^2_{real}=0.91 R^2_{random}=0.65

Fig. 2D p=0.0087 R^2_{real}=0.80 R^2_{random}=0.45

For the results in Fig. 3, we give a typical example for Colombia:

Fig. 3 p=0.0018 R^2_{real}=0.83 R^2_{random}=0.40

We have investigated other null model variants and found similar results, confirming the non-trivial nature of our findings. Examples of the R^2 histograms for these randomized series for Fig. 2A (left) and 3 for Colombia (right) are:

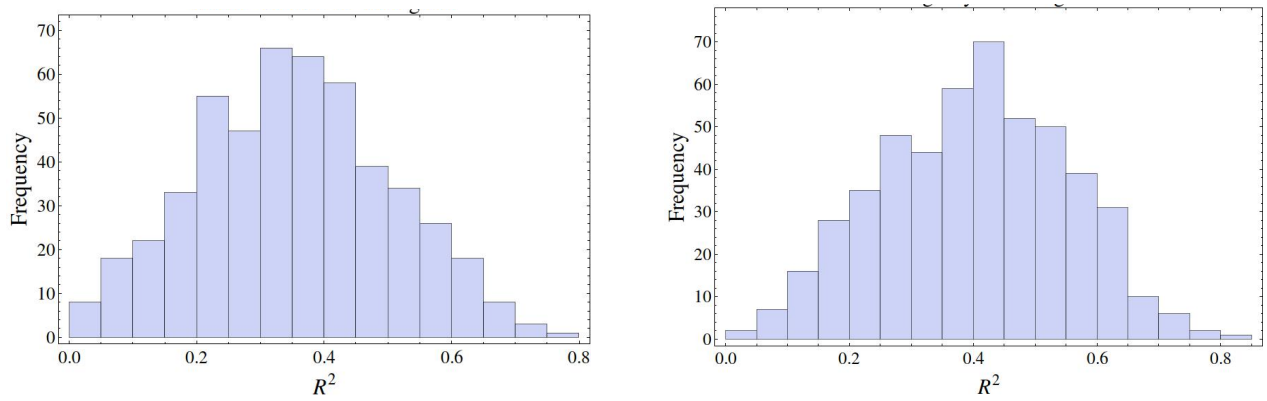

Fig. S10. Distribution of R^2 results. Left: results for randomized series of Colombia events. Right: actual results for Colombia events.

Below is an explicit example for Fig. 2C, comparing real (left) and randomized (right) versions:

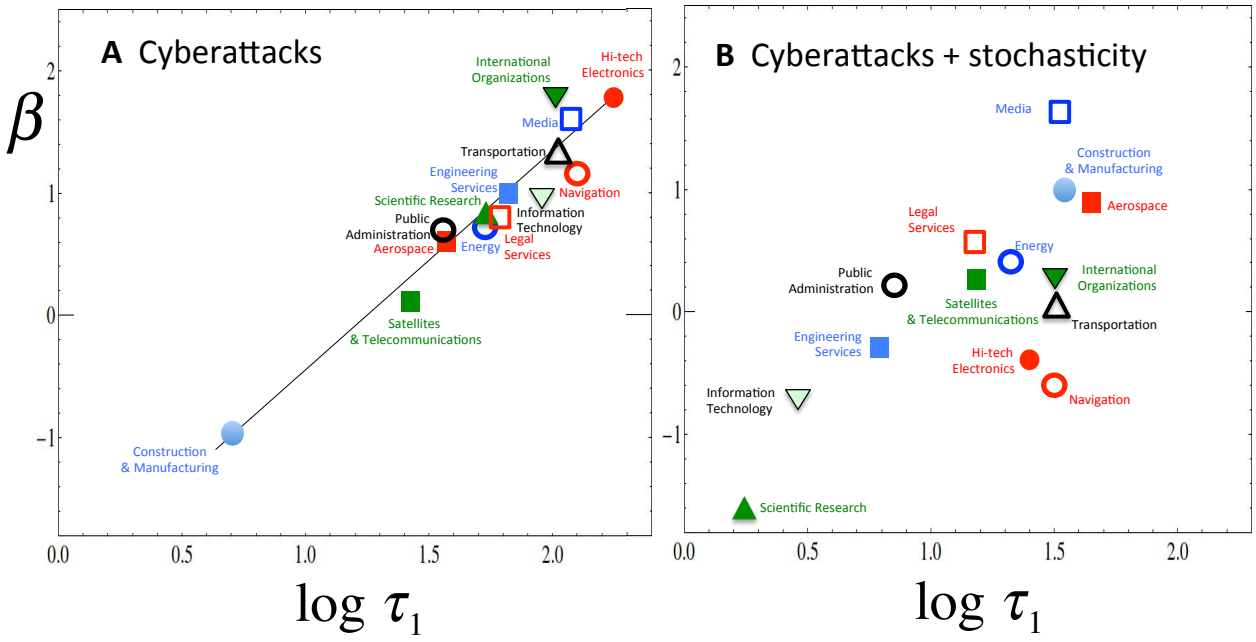

Fig. S11. Examining effects of randomization on results for timings in main paper. Left: actual results for Fig. 2C. Right: results for randomized event series for Fig. 2C.

For completeness, we now discuss some other candidate mechanisms that one might propose to explain the timings signature that we observe, but which can also be rejected by comparison with the actual results:

(1) Concerning the resolution of the data for insurgencies, fatal days are by definition one day or more apart. One might wonder if this finite data resolution affects our results, and hence generates a false correlation between β and $\log \tau_1$ due to accumulation of $\tau_n = 1$ values. For most dyads, as can be seen explicitly for the example above of Magdalena, this is not an issue since the $\tau_n = 1$ values are very infrequent. Even when they do occur, the $\tau_n = 1$ values tend to be real and not a spurious resolution effect. We have checked that our results are insensitive to whether they are included in the dataset or not. For the cases that $\tau_n = 1$ values do begin to accumulate, we truncate the dataset at a value $n_{\max}$ and obtain the best-fit power-law curve for $n \le n_{\max}$. To deduce which $n_{\max}$ value to use, we employ an algorithm that detects the onset of any accumulation based on a moving average. We checked the robustness of our results to variations of this algorithm. Alternative algorithms such as LOWESS give similar results. The robustness of our findings in the case of Afghanistan, mentioned in the main paper, is discussed in more detail in the online preprint http://arxiv.org/abs/1109.2076 ("Escalation, timing and severity of insurgent and terrorist events: Toward a unified theory of future threats").

(2) Start with the assumption that the set of $\{\tau_n\}$ data for each dyad follows the power-law curve and that on the log-log plot it follows a straight line with Gaussian-distributed i.i.d. residuals. We know this is consistent with the real data (e.g. Magdalena shown above) but now let's assume momentarily that it also happens for data generated by a null model in order to see how this might favour a candidate null model explanation of our results. Each data-point can therefore be written as $\log \tau_n = \log \tau_1 - \beta \log n + \varepsilon_n$. Adding together over all N data-points yields

$\sum_{n=1}^{N} \log\ \tau_n = \sum_{n=1}^{N} \log\ \tau_1 - \beta \sum_{n=1}^{N} \log n$ assuming that the residuals add to give approximately zero. This can then be rewritten as $\sum_{n=1}^{N} \log\ \tau_n = N \log\ \tau_1 - \beta \log \prod_{n=1}^{N} n$. Rearranging yields $\beta = \left(\frac{N}{\log N!} \right) \log\ \tau_1 - \frac{\log \prod_{n=1}^{N} \tau_n}{\log N!}$. One might wonder if this equation explains Figs. 2 and 3. It does not: Each dyad in a given domain has a distinct numbers of events, and hence a distinct number N of inter-event time intervals. Hence the factors $\log N!$ and N differ between dyads. The factor $\prod_{n=1}^{N} \tau_n$ also differs between dyads. Hence β is not a priori proportional to $\log\ \tau_1$. If a null model constructs each dyad $\left(\log\ \tau_1, \beta\right)$ value by drawing N (i.e. the specific number of $\{\tau_n\}$ for that dyad) values from a stationary distribution of time intervals, it will not reproduce the same scatter of β vs. $\log\ \tau_1$ points that we see in the main paper. We can show this more explicitly by writing $\log\ \tau_n = \log\ \bar{\tau} + \varepsilon_n$ where $\bar{\tau}$ is the mean of the null model distribution and ε_n is a stochastic term with zero mean. Substituting into the above equation yields $\beta = \left(\frac{N}{\log N!} \right) \varepsilon_1$ assuming the sum of the stochastic terms is negligibly small. In general, since N differs between dyads, this does not produce a straight line. If we momentarily assume that N is the same for each dyad (which it is not), a straight line appears – however, it is still not the same straight line scatter of points as in Figs. 2 and 3. Since ε_1 is equally likely to be positive or negative, it produces a straight line scatter which is symmetric around $\beta = 0$ with both positive and negative values, however this is not the case in Figs. 2 and 3 in general. The value of the slope $\left(\frac{N}{\log N!} \right)$ is also different from the one we observe, and it tends toward zero as N increases. The underlying assumption of drawing $\{\tau_n\}$ from a stationary distribution also ignores the fact that in the individual progress curve plots of $\log\ \tau_n$ vs. $\log n$ (see above for Magdalena, Colombia) there is typically a visible linear trend in the τ_n values. Although there is scatter about this linear trend, large values of τ_n tend to occur earlier on in the series (giving $\beta > 0$), or later on in the series ($\beta < 0$), making the null model assumption of a stationary distribution very hard to justify. Generating a model by shuffling $\{\tau_n\}$ values with replacement, produces similar conclusions, and it has an additional lack of realism in that the corresponding distribution only contains these specific τ_n values, i.e. for some unknown reason, these τ_n values are suddenly the only τ_n values allowed. A model generated by shuffling without replacement is even more inappropriate as a plausible explanation, since it implies there is some memory process at work in all domains whereby the system can remember past values of τ_n and not re-use them. Indeed any such shuffling scheme of τ_n to form a candidate null model, is hard to justify since it does not correspond to randomizing event times. Perhaps most importantly, the explanatory power of all such models involving randomization is severely compromised by the fact that the information about the ordering of individual dyads along the line is lost, and hence the relative locations of the dyads along the line will typically bear no relation to the actual ones in Figs. 2 and 3. This can be seen in the figure above when compared to Fig. 2C. Such a null model

cannot therefore reproduce the meaningful insights mentioned in association with the actual data in the main paper, e.g. a super-linear escalation $(\beta > 1)$ for cyber-attacks against international organizations, high-tech electronics and the media, as compared to de-escalation $(\beta \approx -1)$ for the construction industry. The null model that is least unrealistic from a mechanistic perspective, given the features of the real systems, is one where the clock times of the actual events themselves are randomized – this is the null model that was discussed above and that was rejected based on the p-significance values.

6. Demonstration of prediction of timing of future events

Below we illustrate the accuracy of out-of-sample predictions, using the timings benchmark of the main paper, for future fatal attacks on Blue (coalition military) in Afghanistan. The only input is the time interval τ_1 between the first two attacks that have been observed to date in a given region X (e.g. Kandahar) that was previously quiet. In the absence of any benchmark, it would be impossible to obtain a projection forward of future time intervals (and hence times) of attacks since there are an infinite number of lines that can be drawn through one point. However, assuming that the same Red underlies the attacks in all these different regions, we can use the linear relation between β and $\log \tau_1$ for all the other regions that have already had attacks in the recent past, but obviously we do *not* include region X in this plot since we are trying to predict future attacks in X. So we use the actual time interval between the first two events as an estimate of the intercept, and then read off β from the linear relationship. Then using $\tau_1 n^{-\beta}$ we can estimate any future time-interval, and hence obtain a prediction for the time of any future attack.

The figure below shows: (a) The predicted (red diamonds) time of the *n*'th future attack compared to the actual time (blue squares) measured in days (vertical scale) since the initial day on which there was a military IED fatality in Kandahar. Horizontal axis is attack label *n*. Predictions are made at the start, and no updating is allowed. An interval of 3 years is shown on the vertical time axis to highlight the long-term nature of the prediction. (b) Comparison of predicted time intervals to the actual ones. Red line is a guide to the eye. (c) Same as (a) but for Kabul. (d) Same as (a) but for Farah, and now including all hostile military fatalities (i.e. fatalities attributed to insurgent activity).

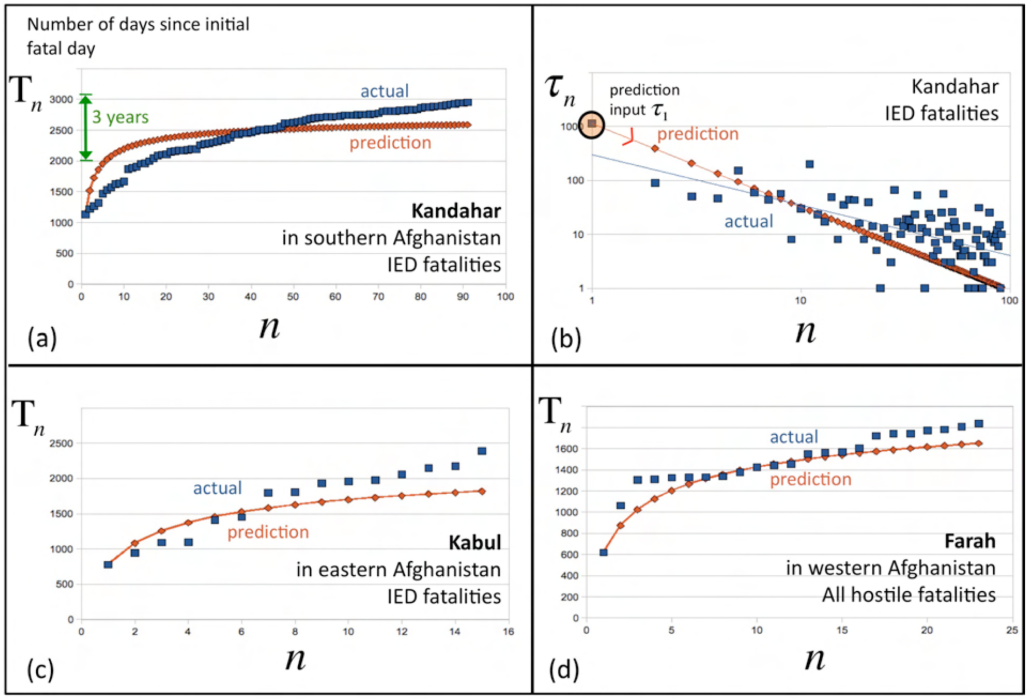

Fig. S12. Results for prediction of future attacks using only one point as input (i.e. initial time-interval). Top left: results for successive attacks *n* in Kandahar against coalition forces, shown as function of calendar time (vertical axis). Top right: underlying plot for successive time-intervals. Bottom left: Similar results for Kabul as a function of calendar time (vertical axis). Bottom right: Similar results for Farah.

7. Additional important references

We note the following additional references which could not be included in the main paper because of space restrictions, but which provide important detailed discussions of particular confrontations or aspects related to the main discussion in the paper:

1. Robb, J.: Brave New War: The Next Stage of Terrorism and the End of Globalization. Wiley, New York (2007)
2. Hammes, T.X.: The Sling and the Stone, on War in the 21st Century. Zenith, St. Paul (2004)
3. Gambetta, D.: Codes of the Underworld: How Criminals Communicate. Princeton University Press, Princeton (2009)
4. The globalization of crime: a transnational organized crime threat assessment, 2010, United Nations Office on Drugs and Crime United Nations publication No. E.10.IV.6. ISBN 978-92-1-130295-0
5. Raab, J., Milward, H.B.: Dark networks as problems. J. Public Adm. Res. Theory **13**, 413 (2003)
6. Stewart, S.: Defining Al Qaeda, Stratfor's Security Weekly, Oct 18, 2012
7. Cederman, L.: Modeling the size of wars: from billiard balls to sandpiles. Am. Polit. Sci. Rev. **97**, 135 (2003)
8. Hedstrom, P., Ylikoski, P.: Causal mechanisms in the social sciences. Annu. Rev. Sociol. **36**, 49 (2010)
9. Norkus, Z.: Mechanisms as miracle makers? The rise and inconsistencies of the 'mechanismic approach' in social science and history. Hist. Theory **44**, 348 (2005)

10. Eguiluz, V.M., Zimmerman, M.G.: Transmission of information and herd behavior. Phys. Rev. Lett. **85**, 5659 (2000)
11. D'Hulst, R., Rodgers, G.J.: Exact solution of a model for crowding and information transmission in financial markets. Int. J. Theor. Appl. Finance **3**, 609 (2000)
12. Axelrod, R.: The dissemination of culture: a model with local convergence and global polarization. J. Confl. Resolut. **41**, 203 (1997)
13. Centola, D., González-Avella, J.C., Eguiluz, V.M., Miguel, M.S.: Homophily, cultural drift, and the co- evolution of cultural groups. J. Confl. Resolut. **51**, 905 (2007)
14. Apolloni, A., Gargiulo, F.: Diffusion processes through social groups' dynamics. Adv. Complex Syst. **14**, 151 (2011)
15. Wyld, A., Rodgers, G.J.: Models for random graphs with variable strength edges. Physica A **374**, 491 (2007)
16. Tadic, B., Rodgers, G.J.: Modelling conflicts with cluster dynamics on networks. Physica A **389**, 5495 (2010)
17. Clauset, A., Wiegel, F.W.: A generalized aggregation-disintegration model for the frequency of severe terrorist attacks. J. Confl. Resolut. **54**, 179 (2010)
18. Kalyvas, S.N.: The Logic of Violence in Civil War. Cambridge University Press, Cambridge (2006)
19. Kalyvas, S.N.: The paradox of terrorism in civil war. J. Ethics **8**, 97 (2004)
20. Bueno de Mesquita, E.: The political economy of terrorism: a selective overview of recent work. Polit. Economist **10**, 112 (2008)
21. Bueno de Mesquita, E.: Conciliation, counterterrorism, and patterns of terrorist violence. Int. Organ. **59**, 145 (2005)
22. Kalyvas, S.N., Kocher, M.A.: The dynamics of violence in Vietnam: an analysis of the Hamlet Evaluation System (HES). J. Peace Res. **46**, 335 (2009)
23. Kaplan, E.H.: Tactical prevention of suicide bombings in Israel (2001–2003). National Academy of Sciences, IED workshops. http://dels.nas.edu/comm/bcst/ieds/pdfs/Kaplan.pdf
24. Kaplan, E.H., Mintz, A., Mishal, S., Samban, C.: What happened to suicide bombings in Israel? Studies in Conflict and Terrorism **28**, 225 (2005)
25. Lyall, J.: Does indiscriminate violence incite insurgent attacks? J. Confl. Resolut. **53**, 331 (2009)
26. Horgan, J.: Divided We Stand: The Psychology and Strategy of Ireland's Dissident Terrorists. Oxford University Press, New York (2013)
27. Carley, K.: Destabilizing terrorist networks. In: Proceedings of the 8th International Command and Con- trol Research and Technology Symposium, National Defense War College, Washington, DC, 2003
28. McCulloh, I.A., Carley, K.M., Webb, M.: Social network monitoring of Al-Qaeda. Network Sci. **1**, 25 (2007)
29. Weinstein, J.M.: Inside Rebellion: The Politics of Insurgent Violence. Cambridge University Press, Cambridge (2007)
30. Cederman, L.E., Gleditsch, K.S.: Conquest and regime change: an evolutionary model of the spread of democracy and peace. Int. Stud. Q. **48**, 603 (2004)
31. Johnson, D.D.P., Tierney, D.: The Rubicon theory of war: how the path to conflict reaches the point of no return. Int. Secur. **36**, 7 (2011)
32. Johnson, D.D.P., Weidmann, N.B., Cederman, L.E.: Fortune favours the bold: an agent-based model reveals adaptive advantages of overconfidence in war. PLoS ONE **6**, e20851 (2011)
33. Drapeau, M.D., Hurley, P.C., Armstrong, R.E.: So many zebras, so little time: ecological models and counterinsurgency operations. Defense Horiz. **62**, 1 (2008)
34. Kress, M.: Modeling armed conflicts. Science **336**, 865 (2012)
35. Epstein, J.: Nonlinear Dynamics, Mathematical Biology and Social Sciences. Addison-Wesley, Reading (1997)
36. MacKay, N.: Lanchester combat models. Math. Today **42**, 170 (2006)
37. Gutfraind, A.: Understanding terrorist organizations with a dynamic model. Studies in Conflict and

Terrorism **32**, 45 (2009)
38. Lim, M., Metzler, R., Bar-Yam, Y.: Global pattern formation and ethnic/cultural violence. Science **317**, 1540 (2007)
39. Forsyth, D.R.: Group Dynamics. Wadsworth, Belmont (2009)
40. Aureli, F., Schaffner, C.M., Boesch, C., Bearder, S.K., Call, J., Chapman, C.A., Connor, R., Di Fiore, A., Dunbar, R.I.M., Henzi, S.P., Holekamp, K., Korstjens, A.H., Layton, R., Lee, P., Lehmann, J., Man- son, J.H., Ramos-Fernandez, G., Strier, K.B., van Schaik, C.P.: Fission–fusion dynamics: new research frameworks. Curr. Anthropol. **49**, 627 (2008)
41. Ispolatov, I., Krapivsky, P.L., Redner, S.: War: the dynamics of vicious civilizations. Phys. Rev. E **54**, 1274 (1996)
42. Caro, T.: Antipredator Defenses in Birds and Mammals. University of Chicago Press, Chicago (2005)

8. Details of the derivation of the Red-Blue relative advantage result quoted in the main paper, which describes and explains the timings benchmark (Figs. 2-3 of main paper); and the derivation of the 2.5 exponent result quoted in the main paper, which describes and reproduces the severity benchmark (Fig. 1 of main paper), using the minimal version of our dynamical clustering theory

The proof of the result $x(n)\big|_{\text{rms}} \propto n^{\beta}$ which is quoted in the main text, is a standard property for stochastic processes, or so-called stochastic 'walks'. We show this here, using slightly different notation, i.e. we call the relative advantage $R(n)$ (i.e. $x(n)$ in the main paper) after n steps. Our notation for the change in $R(n)$ at step i is $\Delta x_i = x_i - x_{i-1}$. Hence the change between step 0 and n is given by $\Delta x_{n,0} = \sum_{j=1}^{n} \Delta x_j = x_n - x_0$. The *mean* change between step 0 and n is:

$$\langle \Delta x_{n,0} \rangle = \sum_{j=1}^{n} \langle \Delta x_j \rangle$$

which is the well-known result that the *average of the sum is equal to the sum of the averages.* This equation holds *irrespective* of whether the changes Δx_j are i.i.d. or not. For the special case in which each mean is always the same $\langle \Delta x_j \rangle \equiv \langle \Delta x \rangle$ (for example, for i.i.d. variables) we have:

$$\langle \Delta x_{n,0} \rangle = \sum_{j=1}^{n} \langle \Delta x_j \rangle = n \langle \Delta x \rangle$$

For the case of the coin-toss walk above, we have $\langle \Delta x \rangle = 0$ where the average includes all possible trajectories for the 'walk'. Hence $\langle \Delta x_{n,0} \rangle = 0$ for all n. The *variance* is as follows:

$$\sigma_{n,0}{}^2 \equiv \left\langle \left(\Delta x_{n,0} - \left\langle \Delta x_{n,0} \right\rangle \right)^2 \right\rangle = \left\langle \left(\Delta x_{n,0} \right)^2 \right\rangle - \left\langle \Delta x_{n,0} \right\rangle^2 = \left\langle \left(\sum_{j=1}^{n} \Delta x_j \right)^2 \right\rangle - \left\langle \sum_{j=1}^{n} \Delta x_j \right\rangle^2$$

$$= \underbrace{\left\langle \sum_{i=1}^{n} \sum_{j=1}^{n} \Delta x_i \Delta x_j \right\rangle}_{\Downarrow} \quad - \quad \underbrace{\left\{ \sum_{j=1}^{n} \left\langle \Delta x_j \right\rangle \right\}^2}_{\Downarrow}$$

$$\sum_{i=1}^{n} \left\langle \left(\Delta x_i \right)^2 \right\rangle + \sum_{i \neq j} \left\langle \Delta x_i \Delta x_j \right\rangle \qquad \sum_{i=1}^{n} \left\langle \Delta x_i \right\rangle^2 + \sum_{i \neq j} \left\langle \Delta x_i \right\rangle \left\langle \Delta x_j \right\rangle$$

Collecting up the cross terms, gives contributions of the form $\left\langle \Delta x_i \Delta x_j \right\rangle - \left\langle \Delta x_i \right\rangle \left\langle \Delta x_j \right\rangle$ which is a crucially important quantity. It connects past outcomes to current outcomes (i.e. Δx_i at step i to Δx_j at step j). It will only be non-zero if there is some kind of memory (i.e. *correlation*) in the process. Specifically, if the changes in the lead Δx_i are *uncorrelated* (i.e. no memory) then $\left\langle \Delta x_i \Delta x_j \right\rangle = \left\langle \Delta x_i \right\rangle \left\langle \Delta x_j \right\rangle$ for $i \neq j$ and hence the above equation simplifies exactly to:

$$\sigma_{n,0}{}^2 = \sum_{i=1}^{n} \left\langle \left(\Delta x_i \right)^2 \right\rangle - \sum_{i=1}^{n} \left\langle \Delta x_i \right\rangle^2 = \sum_{i=1}^{n} \left\{ \left\langle \left(\Delta x_i \right)^2 \right\rangle - \left\langle \Delta x_i \right\rangle^2 \right\} = \sum_{i=1}^{n} \sigma_{i,i-1}{}^2$$

Hence we have proved the well-known statistical result for *uncorrelated* variables (i.e. no memory) that the *variance of the sum is equal to the sum of the variances.* For the special case in which each variance is the same for each step (for example, for i.i.d. variables) then $\sigma_{i,i-1}{}^2 \equiv \sigma^2$ and we have:

$$\sigma_{i,i-n}{}^2 \equiv \sum_{i=1}^{n} \sigma_{i,i-1}{}^2 = n \sigma^2$$

where $\sigma_{i,i-n}{}^2 = \sigma_{n,0}{}^2$ since the lead-changes at each step have the same variance. Taking the square root of each side, this gives the result quoted in the main paper that the typical size (i.e. root-mean-square 'rms') of an uncorrelated process following the *n*'th attack (recall each attack is a step in the walk) increases as n^{β} where $\beta = 0.5$. Using the more general notation of this SI, we have:

$$\sigma_{i,i-n} = n^{\frac{1}{2}} \, \sigma$$

So, *the typical size of the lead of Red over Blue (or vice versa) for the entire confrontation to date, with n attacks to date, increases as the square-root of n, i.e. n to the power 0.5, when the process is uncorrelated*. For the special case of a coin-toss walk, we have $\sigma = d$ and hence $\sigma_{i,i-n} = n^{\frac{1}{2}} \, d$.

We stress that the timestep here, i.e. the tick of the clock from *n* to *n*+1, is measured on an event clock, not a time clock. In the more general case of a positive correlation (i.e. some memory), the corresponding expression for the typical size of R (i.e. root-mean-square) will therefore be larger than the uncorrelated case of $n^{\beta=0.5}$, i.e. $\beta > 0.5$ in the notation of the main paper. By contrast, if the changes Δx_i are *anti-correlated* (i.e. their correlation is negative), then the dependence will approach n^0, i.e. $0 < \beta < 0.5$ in the notation of the main paper.

Hence in general (i.e. in the presence of correlations) the relative advantage will have the property that the typical size after n events, given by $x(n)\big|_{\text{rms}}$, increases as n^{β} as we claimed.

Our theoretical explanation of the timings, discussed in the main paper, can also be extended to explain the typical scatter of observed time-interval values around the best-fit progress curve shown in Fig. 3 (top inset) if we assume that a series of steps need to happen before Red can complete its next attack against Blue. Each of these steps may fall behind or ahead of schedule for multiple external reasons, e.g. protest members may be unable to continue coordinating or insurgents may not receive new ammunition. Following multiplicative degradation processes in engineering, we assume each of these steps multiplies the expected time interval by a factor $\left(1+\varepsilon_j\right)$ where the ε_j's are Gaussian distributed i.i.d. stochastic variables which mimic these exogenous factors. Hence the observed time interval is given by $\tau_1 n^{-\beta}\prod_{j=1}^{N}\left(1+\varepsilon_j\right)$. Taking the logarithm of both sides, and assuming $\varepsilon_j \ll 1$ gives a straight line fit on a log-log plot as observed in Fig. 3 (upper inset) and with Gaussian-distributed i.i.d. residuals, as we observe empirically (see figure in Section 4 of this SI).

We now turn to the distribution of severities in Fig. 1, and our claim in the main paper that $\alpha \sim 2.5$. We stress that even though the overall command structure of Red might be hierarchical, or portrayed as so to give the impression of a strong army, our theory aligns with the PIRA analysis and other recent fieldwork studies by Kenney, Gambetta et al. in finding that the *operational* structure is delocalized into clusters. Our dynamical clustering theory for Red is exactly solvable at the level of mean-field theory, which means that the equations that are written down to denote the change in the average number of clusters of a given size, per timestep, is exactly solvable.

As shown later in this section, each cluster-size has its own equation, and they are coupled – however use of a generating function approach enables an exact solution. Many variants can also be solved exactly. Below we provide a list of results for the model and its variants, with Blue referred to as A and Red referred to as B. This table shows the robustness of the results as generalizations are made. For details of certain generalizations, see Ruszczycki, B., Zhao, Z., Burnett, B., Johnson, N.F.: Relating the microscopic rules in coalescence-fragmentation models to the cluster-size distribution. Eur. Phys. J. B **72**, 289 (2009). Also see Clauset, A., Wiegel, F.W.: A generalized aggregation-disintegration model for the frequency of severe terrorist attacks. J. Confl. Resolut. **54**, 179 (2010).

Model variants	Description of model variant			Effect of heterogeneity in character of individuals?	Proof of results requires computer simulations?	Consistent with empirical results for severity of violence?
	Armed population B (e.g. insurgency)	Armed population A (e.g. army)	Unarmed population C (e.g. civilians)			
1.0	**Dynamical clustering of B agents (which is equivalent to a dynamical network). Each cluster has probability ν_{coal} of coalescing with another cluster, and probability ν_{frag} of fragmenting. Size of B population N is constant, but total number of B clusters $N_{\text{clusters}}(t)$ varies endogenously in time *t***	**Inert. Population A simply triggers sporadic fragmentation of B clusters. Mimics agents breaking contacts/fleeing when in danger**	**Inert. Incurs casualties proportional to size of insurgent clusters**	**No effect if ν_{coal} and ν_{frag} do not depend on character variables**	**NO All analytic. Detailed derivation given in SI below**	**YES** **Produces power-law $p(x) \propto x^{-\alpha}$ with $\alpha = 2.5$ for $x > x_{\min}$, independent of *N*. Exponential cutoff at large x due to finite population size *N*. $\alpha = 2.5$ result emerges for a range of values of ν_{coal} and ν_{frag}, hence this is not just a typical phase transition effect from statistical mechanics in which the system needs to be tuned to the phase transition**
1.1	Same as 1.0 except multiple clusters may coalesce at any one time	Same as 1.0	Same as 1.0	Same as 1.0	NO	**YES** $\alpha = 2.5$. Same as 1.0
1.2	Same as 1.0 except fragment size x_0 may be larger than 1, as long as $x_0 << N$	Same as 1.0	Same as 1.0	Same as 1.0	NO	**YES** $\alpha = 2.5$. Same as 1.0 but $x_{\min} > x_0$
1.3	Same as 1.0 except size of population *N* may fluctuate in time	Same as 1.0	Same as 1.0	Same as 1.0	Some analytic results possible	**YES**. $\alpha = 2.5$ as long as fluctuations small compared to *N* and slow compared to coalescence-fragmentation rates. Exponential cut-off and onset $x_{\min}$ may fluctuate in time.
2.0	Similar to 1.0 but agents located at vertices of a spatial grid in *D*-dimensions. Model 1.0 corresponds to $D \to \infty$	Same as 1.0	Same as 1.0	Same as 1.0	Some analytic results possible	**YES**. α varies from $\alpha = 1.9$ for $D = 2$, up to $\alpha = 2.5$ for $D \to \infty$
3.0	Similar to 1.0 but rigidity of clusters (i.e. probability of a picked cluster *i* coalescing or fragmenting) depends on size according to $x_i^{-\delta}$ where δ can be positive or negative.	Same as 1.0	Same as 1.0	Same as 1.0	NO	**YES.** Similar to 1.0, but $\alpha = 2.5 - \delta$ so α takes on range of values around 2.5, as observed empirically, according to magnitude and sign of δ, e.g. $1.8 < \alpha < 3.2$ for $0.7 > \delta > -0.7$. Implication is that conflicts with different α values around 2.5, differ primarily in the relative rigidity of their B population's (e.g. insurgent) clusters
4.0	Similar to 1.0 but vector with bit string defines individual agent character. Coalescence-fragmentation probability depends on similarity of vectors	Same as 1.0	Same as 1.0	Yes. Similarity of vectors favors cluster formation	Some analytic results possible	**YES.** $\alpha = 2.5$
5.0	Similar to 1.0 but scalar number $0 \le p \le 1$ defines individual agent character. Similarity of *p* values favors cluster formation	Same as 1.0	Same as 1.0	Yes. Mimics KINSHIP	NO	**YES.** $\alpha = 2.5$ but phase transition observed for particular $p \equiv p_{c,\text{kinship}}$. Regime $p < p_{c,\text{kinship}}$ is dominated by isolated agents (e.g. insurgent clusters hardly ever form)
5.1	Similar to 5.0 but dissimilarity of *p* favors cluster formation	Same as 1.0	Same as 1.0	Yes. Mimics TEAM FORMATION	NO	**YES.** $\alpha = 2.5$ Similar to 5.0. but $p_{c,\text{team}} \neq p_{c,\text{kinship}}$
5.2	Intermediate between 5.0 and 5.1	Same as 1.0	Same as 1.0	Yes. MIXED	NO	**YES.** $\alpha = 2.5$ Similar to 5.0. $p_{c,\text{mixed}} \neq p_{c,\text{team}} \neq p_{c,\text{kinship}}$
6.0	Populations A,B both dynamically clustering. Coalescence/fragmentation dictated by size of A and B clusters in individual clashes	Dynamically clustering	Same as 1.0	Possible, but no character effects included so far	Depends on cluster-cluster interaction rules	**YES.** Can produce distributions for A and B casualties consistent with observed values of $\alpha = 2.5$, and goodness-of-fit values from 0 to 1 as observed
7.0	Populations A, B, C all dynamically clustering. Coalescence/fragmentation dictated by size of A, B and C clusters in individual clashes	Dynamically clustering	Dynamically clustering	Possible, but no character effects included so far	Depends on cluster-cluster interaction rules	**YES.** Can produce distributions for A, B and C casualties consistent with observed values of $\alpha = 2.5$, and goodness-of-fit values from 0 to 1 as observed

Table S1. Effect of generalizations of simple one-population coalescence-fragmentation model from main paper, describing Red.

It is straightforward to also implement this clustering theory using a simulation. On each timestep, a Red member (and hence the cluster to which this person belongs) is selected at random, for example through some process in which he/she gains some information about an opportunity or an impending attack by Blue. This is equivalent to saying a cluster is selected with probability proportional to its size. The cluster to which the agent belongs may then fragment, if it senses danger for example. It may also coalesce, or simply remain unchanged.

In what follows we show how our theory derives the $\alpha = 2.5$ benchmark for the event severity distribution in Fig. 1. The Master Equation for the number of clusters of size s is as follows:

$$\frac{\partial n_s}{\partial t} = \frac{\nu_{\rm coal}}{N^2}\sum_{k=1}^{s-1} k n_k (s-k) n_{s-k} - \frac{\nu_{\rm frag} s n_s}{N} - \frac{2\nu_{\rm coal} s n_s}{N^2}\sum_{k=1}^{\infty} k n_k \ , \quad s \geq 2 \ , \tag{1}$$

$$\frac{\partial n_1}{\partial t} = \frac{\nu_{\rm frag}}{N}\sum_{k=2}^{\infty} k^2 n_k - \frac{2\nu_{\rm coal} n_1}{N^2}\sum_{k=1}^{\infty} k n_k \ . \tag{2}$$

Here $\nu_{\rm coal}$ and $\nu_{\rm frag}$ are the probabilities per timestep (i.e. rates) of coalescence of two clusters, or fragmentation of a cluster, respectively. To simplify the limits of the sums, we extend the upper limit to infinity, which is a good approximation for large N. Terms on the right hand side of Eq. (1) represent all the ways in which n_s can change. In the steady state:

$$s n_s = \frac{\nu_{\rm coal}}{(\nu_{\rm frag} + 2\nu_{\rm coal})N}\sum_{k=1}^{s-1} k n_k (s-k) n_{s-k} \ , \quad s \geq 2 \ , \tag{3}$$

$$n_1 = \frac{\nu_{\rm frag}}{2\nu_{\rm coal}}\sum_{k=2}^{\infty} k^2 n_k \ . \tag{4}$$

Consider

$$G[y] = \sum_{k=0}^{\infty} k n_k y^k = n_1 y + \sum_{k=2}^{\infty} k n_k y^k \equiv n_1 y + g[y] \ , \tag{5}$$

where y is a parameter and g[y] governs the cell size distribution n_k for $k \geq 2$. Multiplying Eq. (3) by y^s and then summing over s from 2 to ∞, yields:

$$g[y] = \frac{\nu_{\rm coal}}{(\nu_{\rm frag} + 2\nu_{\rm coal})N} G[y] \ , \tag{6}$$

i.e.

$$g[y]^2 - \left(\frac{\nu_{\rm frag} - 2\nu_{\rm coal}}{\nu_{\rm coal}} N - 2 n_1 y\right) g[y] + n_1^2 y^2 = 0 \ . \tag{7}$$

From Eq. (5), $g[1] = G[1] - n_1$. Substituting this into Eq. (7) and setting $y = 1$, we can solve for $g[1]$

$$g[1] = \frac{\nu_{\rm coal}}{\nu_{\rm frag} + 2\nu_{\rm coal}} N \ . \tag{8}$$

Hence

$$n_1 = N - g[1] = \frac{\nu_{\rm frag} + \nu_{\rm coal}}{\nu_{\rm frag} + 2\nu_{\rm coal}} N \ . \tag{9}$$

Substituting this into Eq. (7) yields

$$g[y]^2 - \left(\frac{\nu_{\rm frag} + 2\nu_{\rm coal}}{\nu_{\rm coal}} N - \frac{2N(\nu_{\rm frag} + \nu_{\rm coal})}{\nu_{\rm frag} + 2\nu_{\rm coal}} y\right) g[y] + \frac{(N(\nu_{\rm frag} + \nu_{\rm coal}))^2}{(\nu_{\rm frag} + 2\nu_{\rm coal})^2} y^2 = 0 \ . \tag{10}$$

We can solve this quadratic for $g[y]$

$$g[y] = \frac{(\nu_{\rm frag} + 2\nu_{\rm coal})N}{4\nu_{\rm coal}} \left(2 - \frac{4(\nu_{\rm frag} + \nu_{\rm coal})\nu_{\rm coal}}{(\nu_{\rm frag} + 2\nu_{\rm coal})^2} y - 2\sqrt{1 - \frac{4(\nu_{\rm frag} + \nu_{\rm coal})\nu_{\rm coal}}{(\nu_{\rm frag} + 2\nu_{\rm frag})^2} y} \right) , \qquad (11)$$

which can be easily expanded

$$g[y] = \frac{(\nu_{\rm frag} + 2\nu_{\rm coal})N}{2\nu_{\rm coal}} \sum_{k=2}^{\infty} \frac{(2k-3)!!}{(2k)!!} \left(\frac{4(\nu_{\rm frag} + \nu_{\rm coal})\nu_{\rm coal}}{(\nu_{\rm frag} + 2\nu_{\rm coal})^2} y \right)^k . \qquad (12)$$

Comparing with the definition of $g[y]$ in Eq. (5) shows that

$$n_s = \frac{\nu_{\rm frag} + 2\nu_{\rm coal}}{2\nu_{\rm coal}} \frac{(2s-3)!!}{s(2s)!!} \left(\frac{4(\nu_{\rm frag} + \nu_{\rm coal})\nu_{\rm coal}}{(\nu_{\rm frag} + 2\nu_{\rm coal})^2} \right)^s . \qquad (13)$$

We now employ Stirling's series

$$ln[s!] = \frac{1}{2} ln[2\pi] + \left(s + \frac{1}{2} \right) ln[s] - s + \frac{1}{12s} - \ldots . \qquad (14)$$

Hence for $s \geq 2$, we find

$$n_s \approx \left(\frac{(\nu_{\rm frag} + 2\nu_{\rm coal})e^2}{2^{3/2}\sqrt{2\pi}\nu_{\rm coal}} \right) \left(\frac{4(\nu_{\rm frag} + \nu_{\rm coal})\nu_{\rm coal}}{(\nu_{\rm frag} + 2\nu_{\rm coal})^2} \right)^s \frac{(s-1)^{2s-3/2}}{s^{2s+1}} N , \qquad (15)$$

which implies that

$$n_s \sim \left(\frac{\nu_{\rm coal}^{s-1}(\nu_{\rm frag} + \nu_{\rm coal})^s}{(\nu_{\rm frag} + 2\nu_{\rm coal})^{2s-1}} \right) s^{-5/2} . \qquad (16)$$

In the limit $s \gg 1$, this is formally equivalent to saying that

$$n_s \sim \exp(-s/s_0) s^{-5/2} \qquad (17)$$

where

$$s_0 = - \left[\ln \left(\frac{4(\nu_{\rm frag} + \nu_{\rm coal})\nu_{\rm coal}}{(\nu_{\rm frag} + 2\nu_{\rm coal})^2} \right) \right]^{-1} \qquad (18)$$

characterizes the exponential cut-off which appears as very high s. The steady state for the distribution of cluster sizes n_s can therefore be considered to be a power-law of the form $\mathrm{M}s^{-\alpha}$ with exponent $\alpha \sim 5/2 = 2.5$, as claimed in the main paper.